

## Double Interpenetration in a Chiral Three-Dimensional Magnet with a (10,3)-a Structure

Thais Grancha,<sup>†</sup> Marta Mon,<sup>†</sup> Francesc Lloret,<sup>†</sup> Jesús Ferrando-Soria,<sup>\*,†</sup> Yves Journaux,<sup>‡</sup> Jorge Pasán,<sup>§</sup> and Emilio Pardo<sup>\*,†</sup><sup>†</sup>Departament de Química Inorgànica, Instituto de Ciencia Molecular (ICMOL), Universitat de València, 46980 Paterna, València, Spain<sup>‡</sup>Institut Parisien de Chimie Moléculaire, Université Pierre et Marie Curie-Paris 6, UMR 7201, F-75252 Paris, France<sup>§</sup>Laboratorio de Rayos X y Materiales Moleculares, Departamento de Física, Universidad de La Laguna, E-38201 Tenerife, Spain

## S Supporting Information

**ABSTRACT:** A unique chiral three-dimensional magnet with an overall racemic double-interpenetrated (10,3)-a structure of the formula  $[(S)-(1\text{-PhEt})\text{-Me}_3\text{N}]_4[\text{Mn}_4\text{Cu}_6(\text{Et}_2\text{pma})_{12}](\text{DMSO})_3 \cdot 3\text{DMSO} \cdot 5\text{H}_2\text{O}$  (1;  $\text{Et}_2\text{pma} = N\text{-}2,6\text{-diethylphenyloxamate}$ ) has been synthesized by the self-assembly of a mononuclear copper(II) complex acting as a metalloligand toward  $\text{Mn}^{\text{II}}$  ions in the presence of a chiral cationic auxiliary, constituting the first oxamato-based chiral coordination polymer exhibiting long-range magnetic ordering.

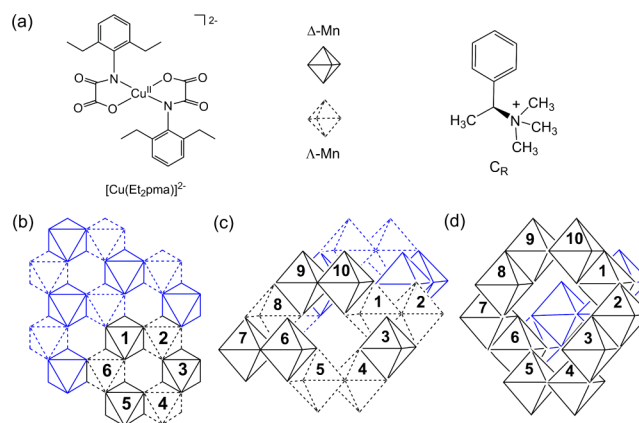
High-dimensional coordination polymers (CPs),<sup>1</sup> sometimes exhibiting fascinating and intriguing interpenetrated architectures,<sup>2</sup> attract the interest of chemists working in very diverse fields because of the broad variety of physical and chemical properties that they can exhibit.<sup>3</sup> The design of CPs exhibiting a spontaneous magnetization below a critical temperature ( $T_C$ )—achieved when suitably chosen paramagnetic ions are linked by appropriate organic ligands (or metalloligands) capable of efficiently transmitting the magnetic coupling between them—is especially appealing in the field of molecular magnetism.<sup>4</sup> In this regard, accurate control of the coordination network structure is required to get the desired long-range magnetic ordering, which is not always easy because of the many subtle factors that may affect the assembly process of the metal and organic building blocks.<sup>5</sup>

With the aim of synthesizing novel examples of heterospin magnets based on CPs, diverse rational self-assembly methods have been proposed that are based on the use of paramagnetic organic radicals or metal complexes as ligands toward other metal ions.<sup>6a</sup> The “complex-as-ligand” approach—where a paramagnetic preformed complex coordinates to free metal ions—has shown excellent results, affording better control of the net topology and the resulting magnetic properties.<sup>6a</sup> In particular, the use of oxamato-based metal complexes as precursors has led to different CPs with a broad diversity of architectures and magnetic properties.<sup>6b</sup>

In a previous work, we showed how the use of tetra-*n*-butylammonium salts of the dianionic mononuclear bis-(oxamato)copper(II) complexes  $(n\text{-Bu}_4\text{N})_2[\text{Cu}^{\text{II}}\text{L}_2]^{2-}$ , where  $\text{L} = N\text{-}2,6\text{-dimethylphenyloxamate}$  ( $\text{Me}_2\text{pma}$ ) and  $N\text{-}2,6\text{-dieth-$

ylphenyloxamate ( $\text{Et}_2\text{pma}$ ) (Scheme 1a), as bis(bidentate) metalloligands toward octahedral manganese(II) cations led to

**Scheme 1.** (a) Mononuclear Copper(II) Complex Anion and Chiral (*S*)-(1-PhEt)Me<sub>3</sub>N Cation and (b–d) Postulated Structures of the Possible Resulting Metal–Organic Frameworks



achiral, either two-dimensional (2D) or three-dimensional (3D),  $\text{Mn}^{\text{II}}_2\text{Cu}^{\text{II}}_3$  extended anionic networks of  $6^3\text{-hcb}$  and  $10^3\text{-ths}$  net topologies, respectively, possessing a regular alternation of propeller-type  $\Delta$ - and  $\Lambda$ - $\text{Mn}^{\text{II}}$  enantiomers (Scheme 1b,c, respectively) and exhibiting long-range magnetic ordering at  $T_C = 10\text{ K}$  (2D) and  $20\text{ K}$  (3D).<sup>7</sup>

With the aim of synthesizing novel examples of chiral oxamato-bridged CPs with additional physical properties to the magnetic ones, which may potentially interact in a synergetic manner, we explore the possibility of achieving CPs with oxamato ligands crystallizing in chiral space groups, which has not been an easy task so far.<sup>8a</sup> So, in order to expand the range of physical properties shown by this class of multifunctional magnetic materials,<sup>6b</sup> we now focus on the use of enantiopure quaternary ammonium cations as chiral auxiliaries such as (*S*)-trimethyl-(1-phenylethyl)ammonium<sup>8b</sup> (Scheme 1a), which can tentatively induce the formation of chiral  $3\text{D Mn}^{\text{II}}_2\text{Cu}^{\text{II}}_3$  extended anionic

Received: July 31, 2015

Published: August 31, 2015



networks of srs net topology possessing a segregated distribution of propeller-type  $\Delta$ - or  $\Lambda$ - $\text{Mn}^{\text{II}}$  enantiomers (Scheme 1d).

Herein we report the synthesis, crystal structure, and magnetic properties of a new example of chiral 3D oxamato-bridged heterobimetallic magnet of the formula  $[(S)-(1\text{-PhEt})\text{-Me}_3\text{N}]_4[\text{Mn}_4\text{Cu}_6(\text{Et}_2\text{pma})_{12}](\text{DMSO})_3 \cdot 3\text{DMSO} \cdot 5\text{H}_2\text{O}$  (**1**). Interestingly, it includes a racemic mixture of double-interpenetrated<sup>2b</sup> 3D  $(\Delta)\text{-Mn}^{\text{II}}_2\text{Cu}^{\text{II}}_3$  and  $(\Lambda)\text{-Mn}^{\text{II}}_2\text{Cu}^{\text{II}}_3$  extended anionic networks, with the source of chirality being provided by the presence of an enantiomerically pure  $(S)-(1\text{-PhEt})\text{Me}_3\text{N}^+$  counteranion.

**1** was obtained by reacting  $[(S)-(1\text{-PhEt})\text{-Me}_3\text{N}]_2[\text{Cu}^{\text{II}}(\text{Et}_2\text{pma})_2] \cdot 4\text{H}_2\text{O}$  and  $\text{MnCl}_2$  (5:1 molar ratio) in a dimethyl sulfoxide (DMSO) solution. **1** crystallizes in the chiral space group  $P2_12_12_1$  of the orthorhombic crystal system, and its absolute configuration was reliably assigned (Table S1 in the Supporting Information, SI).

The structure of **1** consists of two double-interpenetrated oxamato-bridged  $\text{Mn}^{\text{II}}_2\text{Cu}^{\text{II}}_3$  anionic 3D networks with the same  $10^3$  srs net topology but opposite chirality, together with  $(S)-(1\text{-PhEt})\text{Me}_3\text{N}^+$  cations and free  $\text{H}_2\text{O}$  and DMSO molecules (Figures 1 and S1 and S2 in the SI). Both 3D networks are built

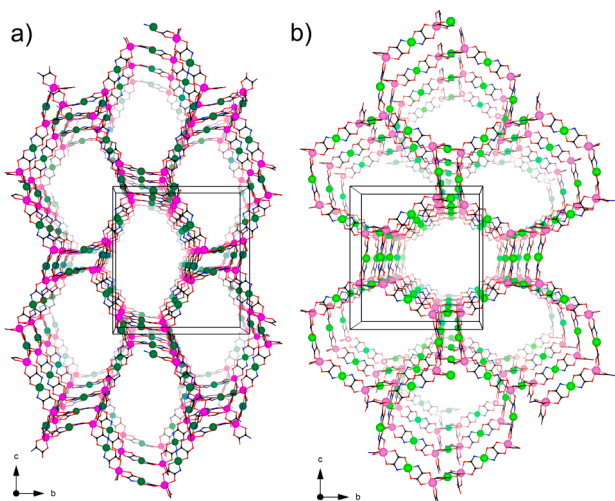


**Figure 1.** Perspective views of the two interpenetrated networks of **1**. The  $(\Delta)\text{-Mn}^{\text{II}}_2(\text{P})\text{-Cu}^{\text{II}}_3$  (a) and  $(\Lambda)\text{-Mn}^{\text{II}}_2(\text{M})\text{-Cu}^{\text{II}}_3$  (b) atoms are depicted in dark and light purple and green colors, respectively. The aromatic rings of the oxamate ligand have been omitted for clarity.

from bis(oxamato)copper(II) entities acting as bis(bidentate) ligands through the *cis*-carbonyl O atoms toward tris(chelated)  $\text{Mn}^{\text{II}}$  ions (Figures 2 and S2 in the SI).

Each network possesses one crystallographically independent Mn atom and three crystallographically independent Cu atoms in the asymmetric unit cell [Mn(1), Cu(1), Cu(2), and Cu(3) in one network and Mn(2), Cu(4), Cu(5), and Cu(6) in the other one]. The Cu atoms are four- and five-coordinate in tetrahedrally distorted square-planar [Cu(1), Cu(3), and Cu(5)] and trigonally distorted square-pyramidal geometries [Cu(2), Cu(4), and Cu(6)], respectively. Their basal plane is formed, in all cases, by two amidate N atoms and two carboxylate O atoms from the *trans*-oxamato groups [Cu–N = 1.887(17)–1.972(17) Å and Cu–O = 1.891(18)–1.976(15) Å]. The apical position of the square-pyramidal  $\text{Cu}^{\text{II}}$  ions is occupied by a DMSO molecule [Cu–O = 2.32(2)–2.471(18) Å]. The values of the tetrahedrality parameter ( $\delta$ ) at the four-coordinate  $\text{Cu}^{\text{II}}$

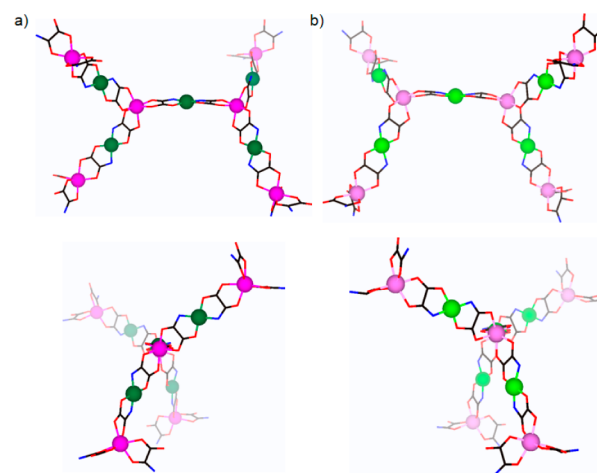


**Figure 2.** Front (top) and side (bottom) views of a fragment of the two interpenetrated networks of **1**. The  $(\Delta)\text{-Mn}^{\text{II}}_2(\text{P})\text{-Cu}^{\text{II}}_3$  (a) and  $(\Lambda)\text{-Mn}^{\text{II}}_2(\text{M})\text{-Cu}^{\text{II}}_3$  (b) atoms are depicted in dark and light purple and green colors, respectively. The aromatic rings of the oxamate ligand have been omitted for clarity.

ions are in the range of 13.7–19.0° ( $\delta = 0$  and 90° for the ideal square plane and tetrahedron, respectively), while those of the trigonality parameter ( $\tau$ ) at the five-coordinate square-pyramidal  $\text{Cu}^{\text{II}}$  ions are in the range of 0.21–0.26 ( $\tau = 0$  and 1 for the ideal square and trigonal bipyramids, respectively). The Mn atoms possess a trigonally distorted octahedral geometry formed by six *cis*-carbonyl O atoms from the oxamato groups [Mn–O = 2.077(18)–2.30(2) Å]. The values of the trigonal twist angle ( $\phi$ ) at the six-coordinate  $\text{Mn}^{\text{II}}$  ions are in the range of 48.2–59.4° ( $\phi = 60$  and 0° for the ideal octahedron and trigonal prism, respectively).

Interestingly, each interpenetrated oxamato-bridged 3D  $\text{Mn}^{\text{II}}_2\text{Cu}^{\text{II}}_3$  anionic network is present as one single enantiomer of opposite chirality, leading to an overall achiral racemic net structure (Figure S2 in the SI). There are previously reported 2-fold interpenetrating srs nets with opposite chirality.<sup>9a</sup> In these cases, the space group is centrosymmetric and the two interwoven 3D nets are related by an inversion center.<sup>9</sup> In **1**, this situation is precluded by the presence of the enantiopure chiral  $(S)-(1\text{-PhEt})\text{Me}_3\text{N}^+$  cations in the pores of the structure and, thus, no inversion centers are allowed. So, each of the two homochiral networks, built by repetition of the nonplanar  $[(\Delta)\text{-Mn}^{\text{II}}_2(\text{P})\text{-Cu}^{\text{II}}_3]$  (Figure 2a) and  $[(\Lambda)\text{-Mn}^{\text{II}}_2(\text{M})\text{-Cu}^{\text{II}}_3]$  (Figure 2b) structural motifs, respectively (with the values of the dihedral angles between the two  $\text{Mn}^{\text{II}}\text{Cu}^{\text{II}}_3$  halves being 74.8 and 75.5°, respectively) is crystallographically unique.

The powder X-ray diffraction pattern of **1** is consistent with the calculated one (Figure S3 in the SI), confirming that the bulk sample is isostructural to the crystal selected for single-crystal X-ray diffraction.

Encouraged by the well-known efficiency of the oxamato ligands transmitting the magnetic coupling between neighboring metal atoms, we studied the magnetic properties of **1**. They are represented in the form of a  $\chi_{\text{M}}T$  versus  $T$  plot [with  $\chi_{\text{M}}$  being the direct-current (dc) molar magnetic susceptibility per  $\text{Cu}_3\text{Mn}_2$  unit and  $T$  the temperature], supporting the occurrence of a 3D ferrimagnetic behavior (Figure 3a). At room temperature,  $\chi_{\text{M}}T$  is equal to 7.97  $\text{cm}^3 \text{mol}^{-1} \text{K}$ . This value is slightly below that expected for the sum of three square-planar  $\text{Cu}^{\text{II}}$  ions ( $\chi_{\text{M}}T = 0.40 \text{ cm}^3 \text{mol}^{-1} \text{K}$  with  $S_{\text{Cu}} = 1/2$  and  $g_{\text{Cu}} = 2.1$ ) and two octahedral high-spin  $\text{Mn}^{\text{II}}$  ions ( $\chi_{\text{M}}T = 4.37 \text{ cm}^3 \text{mol}^{-1} \text{K}$  with

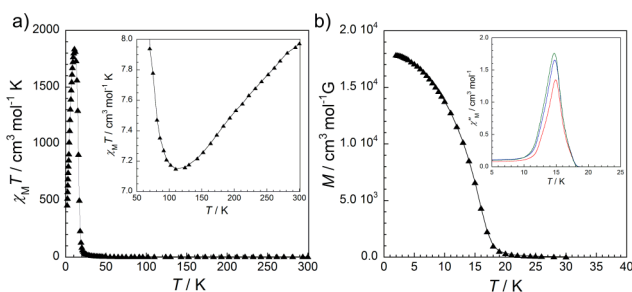


**Figure 3.** (a) Temperature dependence of  $\chi_M T$  for **1** under an applied dc field of 0.1 kG ( $T < 50$  K) and 10 kG ( $T \geq 50$  K). The inset shows the minima in detail. (b) FCM for **1**, measured upon cooling within a field of 100 G. The inset shows the temperature dependence of  $\chi_M''$  with a 1.0 G oscillating field at different frequencies: 10 (red), 100 (blue), and 1000 (green) Hz. The solid lines are only guides for the eye.

$S_{\text{Mn}} = 5/2$  and  $g_{\text{Mn}} = 2.0$ ), suggesting the occurrence of a moderate intramolecular antiferromagnetic interaction between the  $\text{Cu}^{\text{II}}$  and  $\text{Mn}^{\text{II}}$  ions through the oxamate bridges. Upon cooling,  $\chi_M T$  slowly decreases and attains a minimum at ca. 110 K (inset of Figure 3a), supporting the occurrence of a 3D ferrimagnetic behavior. Further cooling shows an abrupt increase of  $\chi_M T$  below 25 K, to reach a maximum value of  $1835 \text{ cm}^3 \text{ mol}^{-1} \text{ K}$  at ca. 11 K.

In fact, **1** undergoes an abrupt paramagnetic-to-ferrimagnetic phase transition at  $T_C = 15$  K, as revealed by the temperature dependence of the field-cooled magnetization (FCM; Figure 3b). The FCM curve, measured by cooling the sample within a small field of 100 G, increases sharply below 20 K, thereby suggesting the onset of a long-range ferrimagnetic transition. Indeed, the magnetic ordering is confirmed by the alternating-current (ac) magnetic properties in the form of the  $\chi_M''$  versus  $T$  plot (with  $\chi_M''$  being the ac out-of-phase susceptibility per  $\text{Cu}_2\text{Mn}_2$  unit) at different frequencies ( $\nu$ ) of the 1 G oscillating field. So,  $\chi_M''$  becomes nonzero below 20 K, and nonfrequency-dependent maxima are observed at 15 K (inset of Figure 3b). The magnetic hysteresis loop at 2.0 K (Figure S4 in the SI) exhibits a very low value of the coercive field ( $H_c = 20$  G), which is characteristic of soft magnets.<sup>6</sup>

In conclusion, a preformed mononuclear copper(II) complex with a chiral counteranion has been used toward  $\text{Mn}^{\text{II}}$  ions to yield the first oxamato-based chiral 3D magnet. Although its structure consists of two enantiopure double-interpenetrated oxamato-bridged  $\text{Mn}^{\text{II}}_2\text{Cu}^{\text{II}}_3$  anionic 3D networks with the same  $10^3$  srs net topology and opposite chiralities, **1** is chiral and crystallizes in a chiral space group as a consequence of the enantiopurity of the auxiliary (*S*)-(1-PhEt) $\text{Me}_3\text{N}^+$  counteranions. Moreover, the presence of long-range ferrimagnetic ordering at 15 K, together with a chiral space group, opens the gate for the observation of interesting properties such as magnetically induced second-harmonic-generation<sup>10a</sup> or magneto-chiral-dichroism<sup>10b</sup> effects. Our current efforts are devoted to the study of these properties in these types of materials.

## ■ ASSOCIATED CONTENT

### ■ Supporting Information

The Supporting Information is available free of charge on the ACS Publications website at DOI: 10.1021/acs.inorgchem.5b01738.

CIF file (CCDC 1416018) (CIF)

Experimental preparation, analytical and spectroscopic characterization of compound **1**, and additional figures (S1–S3) (PDF)

## ■ AUTHOR INFORMATION

### Corresponding Authors

\*E-mail: [jesus.ferrando@uv.es](mailto:jesus.ferrando@uv.es).

\*E-mail: [emilio.pardo@uv.es](mailto:emilio.pardo@uv.es).

### Notes

The authors declare no competing financial interest.

## ■ ACKNOWLEDGMENTS

This work was supported by MINECO (Projects CTQ2013-46362-P and CTQ2013-44844-P) and the Generalitat Valenciana (Project PROMETEOII/2014/070). T.G. and M.M. thank the Universitat de Valencia and MINECO for predoctoral contracts. Thanks are also extended to the MICINN Ramón y Cajal Program (E.P.).

## ■ REFERENCES

- (1) Abrahams, B. F.; Hoskins, B. F.; Michail, D. M.; Robson, R. *Nature* **1994**, *369*, 727–729.
- (2) (a) Batten, S. R.; Robson, R. *Angew. Chem., Int. Ed.* **1998**, *37*, 1460–1494. (b) Han, L.; Qin, L.; Xu, L. P.; Zhao, W. N. *Inorg. Chem.* **2013**, *52*, 1667–1669.
- (3) (a) Li, J.-R.; Kuppler, R. J.; Zhou, H.-C. *Chem. Soc. Rev.* **2009**, *38*, 1477–1504. (b) Gascon, J.; Corma, A.; Kapteijn, F.; Llabrés i Xamena, F. X. *ACS Catal.* **2014**, *4*, 361–378. (c) Train, C.; Gruselle, M.; Verdager, M. *Chem. Soc. Rev.* **2011**, *40*, 3297–3312. (d) Horike, S.; Umeyama, D.; Kitagawa, S. *Acc. Chem. Res.* **2013**, *46*, 2376–2384. (e) Ferrando-Soria, J.; Khajavi, H.; Serra-Crespo, P.; Gascon, J.; Kapteijn, F.; Julve, M.; Lloret, F.; Pasán, J.; Ruiz-Pérez, C.; Journaux, Y.; Pardo, E. *Adv. Mater.* **2012**, *24*, 5625–5629. (f) *Molecule-Based Magnetic Materials*; Turnbull, M. M., Sugimoto, T., Thompson, L. K., Eds.; ACS Symposium Series; American Chemical Society: Washington, DC, 1996; Vol. 644.
- (4) Kahn, O. *Molecular Magnetism*; VCH Publishers: New York, 1993.
- (5) (a) Tabellion, F. M.; Seidel, S. R.; Arif, A. M.; Stang, P. J. *J. Am. Chem. Soc.* **2001**, *123*, 7740–7741. (b) Goesten, M. G.; Kapteijn, F.; Gascon, J. *CrystEngComm* **2013**, *15*, 9249–9257.
- (6) (a) Pardo, E.; Ruiz-García, R.; Cano, J.; Ottenwaelde, X.; Lescouëzec, R.; Journaux, Y.; Lloret, F.; Julve, M. *Dalt. Trans.* **2008**, *21*, 2780–2805. (b) Grancha, T.; Ferrando-Soria, J.; Castellano, M.; Julve, M.; Pasán, J.; Armentano, D.; Pardo, E. *Chem. Commun.* **2014**, *50*, 7569–7585.
- (7) Ferrando-Soria, J.; Grancha, T.; Julve, M.; Cano, J.; Lloret, F.; Journaux, Y.; Pasán, J.; Ruiz-Pérez, C.; Pardo, E. *Chem. Commun.* **2012**, *48*, 3539–3541.
- (8) (a) Grancha, T.; Tourbillon, C.; Ferrando-Soria, J.; Julve, M.; Lloret, F.; Pasán, J.; Ruiz-Pérez, C.; Fabelo, O.; Pardo, E. *CrystEngComm* **2013**, *15*, 9312–9315. (b) Clemente-Leon, M. *Inorg. Chem.* **2008**, *47*, 6458–6463.
- (9) (a) Carlucci, L.; Ciani, G.; Proserpio, D. M.; Sironi, A. *Chem. Commun.* **1996**, 1393–1394. (b) Alexandrov, E. V.; Blatov, V. A.; Kochetkov, A. V.; Proserpio, D. M. *CrystEngComm* **2011**, *13*, 3947–3958.
- (10) (a) Train, C.; Nuida, T.; Gheorghe, R.; Gruselle, M.; Ohkoshi, S. J. *Am. Chem. Soc.* **2009**, *131*, 16838–16843. (b) Train, C.; Gheorghe, R.; Krstic, V.; Chamoreau, L.-M.; Ovanesyan, N. S.; Rikken, G. L. J. a.; Gruselle, M.; Verdager, M. *Nat. Mater.* **2008**, *7*, 729–734.